Received: 17 November 2019 | Revised: 19 January 2020 | Accepted: 17 February 2020

DOI: 10.1002/chir.23209



WILEY

SPECIAL ISSUE ARTICLE

# Furoic acid derivatives from the endophytic fungus *Coniothyrium* sp.

**Nam Michael Tran-Cong**[1] | **Attila Mándi**[2] | **Sándor Balázs Király**[2] | **Tibor Kurtán**[2] | **Wenhan Lin**[3] | **Zhen Liu**[1] | **Peter Proksch**[1]

[1]Institute of Pharmaceutical Biology and Biotechnology, Heinrich Heine University Düsseldorf, Düsseldorf, Germany

[2]Department of Organic Chemistry, University of Debrecen, Debrecen, Hungary

[3]State Key Laboratory of Natural and Biomimetic Drugs, Peking University, Beijing, China

**Correspondence**
Zhen Liu and Peter Proksch, Institute of Pharmaceutical Biology and Biotechnology, Heinrich Heine University Düsseldorf, Universitätsstrasse 1, 40225 Düsseldorf, Germany.
Email: zhenfeizi0@sina.com; proksch@hhu.de

**Funding information**
Deutsche Forschungsgemeinschaft, Grant/Award Numbers: 270650915, GRK 2158, 270650915, GRK 2158; National Research, Development and Innovation Office, Grant/Award Number: K120181; Hungarian Academy of Sciences; Manchot Foundation

**Abstract**

The endophytic fungus *Coniothyrium* sp. was isolated from leaves of *Quercus robur*. Fermentation of this fungus on solid rice medium yielded two new furoic acid derivatives (**1** and **2**) and two additional known compounds. The structures of the new compounds were determined by extensive analysis of 1D and 2D nuclear magnetic resonance spectra as well as high-resolution mass spectrometry data. Compound **1**, containing three aromatic chromophores attached by rotatable sigma bonds and a chirality center in benzylic position, was found to be a scalemic mixture with an excess of the (S) enantiomer, the absolute configuration of which was elucidated as by the solution time-dependent density functional theory-electronic circular dichroism approach. The ωB97X/TZVP PCM/MeCN and SOGGA11-X/TZVP SMD/MeCN methods were used for geometry reoptimization to reproduce the solution conformational ensemble. All isolated compounds were tested for their cytotoxicity but proved to be inactive.

**KEYWORDS**

*Coniothyrium* sp, electronic circular dichroism, furoic acid derivatives, TDDFT-ECD calculation

## 1 | INTRODUCTION

Endophytic fungi are a prominent source for the discovery of new compounds.[1,2] There are an estimated 1.5 million fungal species on Earth, of which only about 70 000 are currently described.[3] Some endophytic fungal genera such as *Aspergillus* and *Penicillium* are well investigated, and their metabolic patterns are well known, even though new compounds are still reported.[4-6] In this study, the endophytic fungus *Coniothyrium* sp. was isolated from leaves of the deciduous tree *Quercus robur*. Literature search for natural products from *Coniothyrium* species revealed several bioactive compounds. Conioimide that was isolated from the Baltic sea alga-derived fungus *Coniothyrium cereale* showed prominent and selective inhibitory activity towards the protease human leukocyte elastase with an $IC_{50}$ value of 0.2 μg/mL.[7] Coniosclerodorolide, a phenalenone derivative, displayed

[This article is part of the Special Issue: In honor and memory of Prof. Koji Nakanishi. See the first articles for this special issue previously published in Volumes 31:12, 32:3, and 32:4. More special articles will be found in this issue as well as in those to come.]

antibacterial activity against *Staphylococcus aureus* SG511 with an MIC value of 24 μM.[8] Coniothyrione, a chlorocyclopentandienylbenzopyrone, was shown to be a bacterial protein synthesis inhibitor and was isolated from *Coniothyrium cerealis* MF7209.[9]

In this study, fermentation of *Coniothyrium* sp. on solid rice medium yielded two new furoic acid derivatives (**1** and **2**) and two additional known compounds 2,3-dihydroxy-2,4-diphenylcyclopent-4-en-1-one (**3**)[10] and 2-anhydromevalonic acid (**4**).[11] The structure elucidation of the new compounds and the results of cytotoxicity assay are described in this paper (Figure 1).

## 2 | MATERIALS AND METHODS

### 2.1 | General experimental procedures

Optical rotations were measured on a PerkinElmer-241 MC polarimeter. 1D and 2D nuclear magnetic resonance (NMR) spectra were recorded with Bruker ARX 300 or AVANCE DMX 600 NMR spectrometers. Mass spectra were obtained from a Finnigan LCQ Deca XP mass spectrometer, while high-resolution mass spectra were recorded by a FTHRMS-Orbitrap (Thermo-Finnigan) mass spectrometer. A Dionex P580 system was used for high-performance liquid chromatography (HPLC) separations in combination with a diode array detector (UVD340S) and an Eurosphere 10 $C_{18}$ column (125 × 4 mm). Semipreparative HPLC was conducted on a Lachrom-Merck Hitachi system (pump L7100, ultraviolet (UV) detector L7400, Eurosphere 100 $C_{18}$ column, 300 × 8 mm, Knauer Germany). Merck MN silica gel 60M (0.04-0.063 mm) was used as stationary phase for column chromatography. TLC plates precoated with silica gel 60 F254 were used for monitoring separation. UV and electronic circular dichroism (ECD) spectra were recorded on a J-810 spectropolarimeter. The HRESIMS, UV, and NMR spectra were included in the Supporting Information.

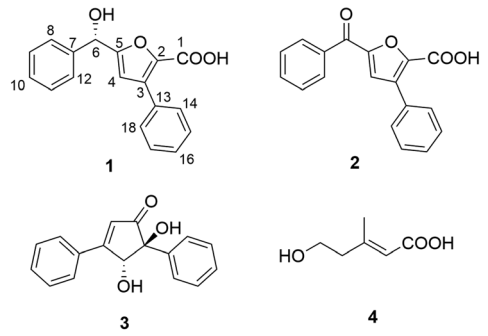


**FIGURE 1** Structures of compounds isolated from *Coniothyrium* sp

### 2.2 | Fungal material and fermentation

Leaves of *Quercus robur* were collected in 2017 in Juelich, Germany. The fresh sample was washed by sterilized water, surface sterilized with 70% ethanol for 1 minute, and cut into small pieces (around 1 × 1 × 1 $cm^3$) using a flame sterilized blade. These pieces were put on malt agar plates (15 g/L malt extract, 15 g/L agar, and 0.2 g/L chloramphenicol in distilled water, pH 7.4-7.8), and then incubated at room temperature for several days. The purified fungus was later transferred to solid rice medium for fermentation. All steps were conducted in an aseptic environment. The identification of the fungus was done using a molecular protocol as described previously.[12] Sequence data were submitted to GenBank with the accession number MN043344. A voucher strain (2BEY) is kept in the Institute of Pharmaceutical Biology and Biotechnology, Heinrich-Heine University, Düsseldorf, Germany.

Large-scale fermentation of this fungus was conducted in five Erlenmeyer flasks on solid rice medium (100 g rice in 110-mL water and autoclaved) at 20°C under static condition. After 20 days, every flask was treated with 600-mL EtOAc and left overnight. Then the EtOAc extract was evaporated under vacuum to obtain the crude extract.

### 2.3 | Isolation of compounds

The crude extract (11.65 g) was subjected to silica gel vacuum liquid chromatography (VLC) using a step gradient of *n*-hexane/EtOAc and $CH_2Cl_2$/MeOH to give 11 fractions (V1-V11). Fraction V4 was further fractionated with RP18-VLC using a gradient of MeOH/$H_2O$ to yield 10 subfractions (V4-1 to V4-10). Compound **3** (6.4 mg) was isolated from subfraction V4-3 by semipreparative HPLC with 30% MeOH/$H_2O$ as mobile phase. Fraction V8 was further subjected to RP18-VLC using a step gradient of MeOH/$H_2O$ to give 10 subfractions (V8-1 to V8-10). Subfraction V8-1 was purified by semipreparative HPLC using 10% MeOH/$H_2O$ to yield **4** (2.1 mg), while subfraction V8-4 was further purified with semipreparative HPLC using 40% MeOH/$H_2O$ to give **1** (1.2 mg) and **2** (2.4 mg).

Coniofuroic acid A (**1**): white amorphous solid; $[\alpha]_D^{20}$ = -4 ($c$ = 0.2 in $CHCl_3$); UV (MeCN) λmax (log ε) 263 (3.41), 221 (3.82) nm; ECD (MeCN, λ [nm] (Δε), c 0.212 mM): 264 (−0.36), 214 (+0.39); $^1H$ and $^{13}C$ NMR see Table 1; high-resolution mass spectrometry (HRMS) (ESI, $m/z$): $[M-H]^-$ calcd for $C_{18}H_{13}O_4$, 293.0814; found 293.0820.

**TABLE 1** $^{1}H$ and $^{13}C$ NMR data of compounds **1** and **2**

| | **1**[a] | | **2**[a] | |
|---|---|---|---|---|
| **No.** | **$\delta_c$ Type**[b] | **$\delta_H$ (*J* in Hz)** | **$\delta_c$ Type**[b] | **$\delta_H$ (*J* in Hz)** |
| 1 | n.d. | | n.d. | |
| 2 | 141.0, C | | 144.7, C | |
| 3 | 135.5, C | | 134.9, C | |
| 4 | 112.1, CH | 6.41, s | 123.4, CH | 7.49, s |
| 5 | 160.8, C | | 152.8, C | |
| 6 | 70.9, CH | 5.81, s | 184.0, C | |
| 7 | 142.3, C | | 137.8, C | |
| 8,12 | 127.9, CH | 7.49, d (8.0) | 130.7, CH | 8.11, d (8.1) |
| 9,11 | 129.5, CH | 7.38, t (8.0) | 129.8, CH | 7.58, t (8.1) |
| 10 | 129.0, CH | 7.32, t (8.0) | 134.4, CH | 7.69, t (8.1) |
| 13 | 133.8, C | | 132.7, C | |
| 14,18 | 130.4, CH | 7.56, d (7.8) | 130.5, CH | 7.66, d (7.9) |
| 15,17 | 128.9, CH | 7.35, t (7.8) | 129.2, CH | 7.42, t (7.9) |
| 16 | 129.1, CH | 7.31, t (7.8) | 129.4, CH | 7.38, t (7.9) |

Abbreviations: HMBC: heteronuclear multiple bond correlation; HSQC: heteronuclear single-quantum correlation; n.d.: not detected; NMR: nuclear magnetic resonance.

[a]Recorded at 600 MHz ($^{1}H$) and 150 MHz ($^{13}C$) in $CD_3OD$.

[b]Data were extracted from HSQC and HMBC spectra.

Coniofuroic acid B (**2**): white amorphous solid; $^{1}H$ and $^{13}C$ NMR see Table 1; HRMS (ESI, *m/z*): $[M - H]^-$ calcd for $C_{18}H_{11}O_4$, 291.0657; found 291.0664.

## 2.4 | Cytotoxicity assay

Cytotoxicity against the L5178Y mouse lymphoma cell line was measured using the MTT assay.[13] Kahalalide F and 0.1% ethylene glycol monomethyl ether in DMSO were used as positive and negative control, respectively.

## 2.5 | Computational methods

Mixed torsional/low-mode conformational searches were carried out by means of the Macromodel 10.8.011 software[14] using the Merck Molecular Force Field (MMFF) with an implicit solvent model for $CHCl_3$ applying a 21 kJ/mol energy window. Geometry reoptimizations of the resultant conformers [ωB97X/TZVP[15] with PCM solvent model for MeCN and SOGGA11-X/TZVP[16] with SMD solvent model for MeCN] and time-dependent density functional theory (TDDFT) calculations were performed with Gaussian 09[17] using various functionals (B3LYP, BH&HLYP, CAM-B3LYP, and PBE0), the TZVP basis set, and the same solvent model as applied in the preceding DFT reoptimization step. ECD spectra were generated as the sum of Gaussians[18] with 3000 $cm^{-1}$ half-height width, using dipole-velocity-computed rotational strengths. Boltzmann distributions were estimated from the ωB97X and the SOGGA11-X energies. The MOLEKEL software package was used for visualization of the results.[19]

## 3 | RESULTS AND DISCUSSION

Compound **1** was isolated as a white amorphous solid. Its molecular formula was determined as $C_{18}H_{14}O_4$ by HRMS, containing 12° of unsaturation. The $^{1}H$ NMR data of **1** showed 11 aromatic protons at $\delta_H$ 7.56 (d, H-14 and H-18), 7.49 (d, H-8 and H-12), 7.38 (t, H-9 and H-11), 7.35 (t, H-15 and H-17), 7.32 (t, H-10), 7.31 (t, H-16), and 6.41 (s, H-4) as well as one oxygenated methine at $\delta_H$ 5.81 (s, H-6) (Table 1). Two monosubstituted benzene rings were assembled by correlation spectroscopy (COSY) correlations between H-8(12)/H-9(11)/H-10 and between H-14(18)/H-15(17)/H-16 together with heteronuclear multiple bond correlation (HMBC) correlations from H-8 to C-10 and C-12, from H-9 to C-7 and C-11, from H-10 to C-8(12), from H-14 to C-16 and C-18, from H-15 to C-13 and C-17, and from H-16 to C-14(18) (Figure 2). The attachment of an oxygenated methine at C-7 was deduced from HMBC correlations from H-6 to C-7 and C-8(12). In addition, HMBC correlations from H-4 to C-2 ($\delta_C$ 141.0), C-3 ($\delta_C$ 135.5), C-5 ($\delta_C$ 160.8), and C-13; from H-6 to C-4 and C-5 ($\delta_C$ 112.1); and from H-14(18) to C-3 indicated the presence of a furan ring and the linkages between C-5/C-6 and C-3/C-13. The location of a carboxy group at C-2 was suggested by the molecular formula of **1**. Thus, the planar structure of **1** was elucidated for which the trivial name coniofuroic acid A is suggested.

For the configurational assignment of **1**, the solution TDDFT-ECD method was applied on the arbitrarily chosen (*S*) stereoisomer.[20,21] Since **1** is conformationally flexible and the relative orientation of the three aromatic chromophores produced by rotation along the C-3-C-13 biaryl axis and the sigma bonds of the C-6 chirality center

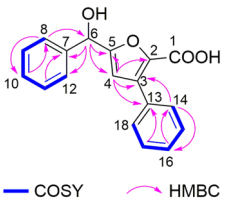


**FIGURE 2** Correlation spectroscopy (COSY) and key heteronuclear multiple bond correlation (HMBC) correlations of compound **1**

is expected to be fundamental for the sign and shape of the ECD transitions, a thorough conformational search is inevitable.[22-25] Consequently, the initial 37 MMFF conformers of (*S*)-**1** were reoptimized at both the ωB97X/TZVP[15] PCM/MeCN and the SOGGA11-X/TZVP[16] SMD/MeCN levels of theory.[26,27] (see Supporting Information) ECD calculations were performed for both sets of conformers at the B3LYP/TZVP, BH&HLYP/TZVP, CAM-B3LYP/TZVP, and the PBE0/TZVP levels with the same solvent model as applied for the preceding DFT reoptimization level. Although as expected the individual conformers gave rather diverse ECD spectra, the Boltzmann-averaged spectra obtained at all applied combinations of levels reproduced well the experimental ECD allowing elucidation of the absolute configuration as (*S*) with high confidence (Figures 3 and 4). The low-energy conformers could be classified into six groups (Figure 5) according to the relative orientation of the three aromatic chromophores, ie, by rotation around the C-3-C-13, C-5-C-6, and C-6-C-7 bonds. The contribution of conformer ingroups A and C with a sum Boltzmann population of 56.6% at the SOGGA11-X/TZVP SMD/MeCN level reproduced already the overall shape of the experimental spectrum (Figure 4). It is also worth to note that the averaged computed ECD spectra obtained at any combinations were much more intense than the experimental one. The experimental ECD spectrum had to be multiplied by 20 to be comparable with the calculated ECD spectra, which implies about more than one order of magnitude difference. This indicated that the sample is probably a scalemic mixture with slight excess

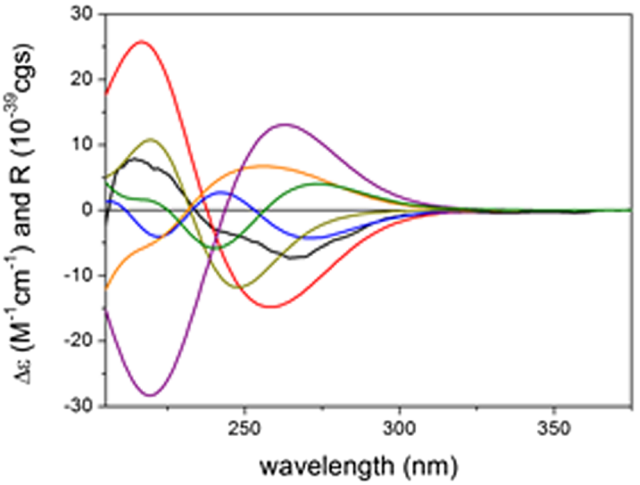


**FIGURE 4** Comparison of the experimental electronic circular dichroism spectrum of **1** (black curve) with the PBE0/TZVP SMD/MeCN spectra of the lowest-energy representative conformers of the six conformational ensembles of (*S*)-**1** (level of optimization: SOGGA11-X/TZVP SMD/MeCN). (red: conf. A, blue: conf. B, olive: conf. G, orange: conf. H, purple: conf. O, green: conf. P.) Sum conformational ensembles were found as group A: 43.3% with conformers A, C, D, F, L, Q, and T; group B: 24.0% with conformers B, E, K, and M; group C: 13.3% with conformers G, I, N, and U; group D: 10.4% with conformers H and J; group E: 3.2% with conformers O and R; group F: 3.1% with conformers P and S

of the (*S*) stereoisome.[28-30] Partial racemization of the chirality center is certainly aided by the benzylic position, since the C-6 chirality center is α position to both a

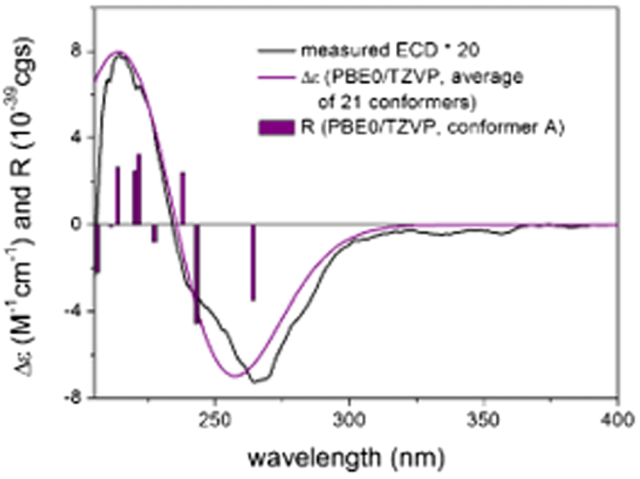


**FIGURE 3** Comparison of the experimental electronic circular dichroism (ECD) spectrum of **1** measured in MeCN (multiplied by 20) with the PBE0/TZVP SMD/MeCN spectrum of (*S*)-**1** (level of optimization: SOGGA11-X/TZVP SMD/MeCN). The bars represent the rotational strength values of the lowest energy conformer

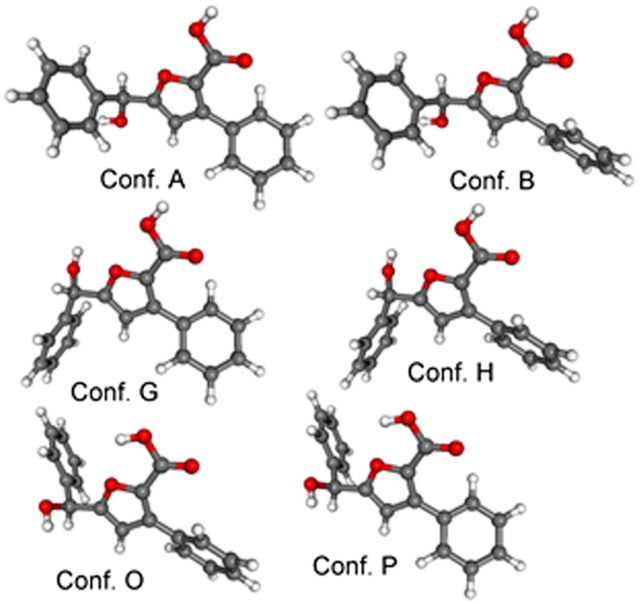


**FIGURE 5** Lowest-energy representatives of the 6 conformer groups of (*S*)-**1**

benzene and a furan ring. For the (*S*) enantiomer of **1**, a relatively strong negative Cotton effect is expected at ~215 nm and a strong positive one at around 265 nm. Although separation of the enantiomers on various chiral HPLC columns was attempted, no successful separation could be achieved with the tested conditions.

The molecular formula of **2** was determined as $C_{18}H_{12}O_4$ based on the HRMS data, lacking two protons when compared to **1**. The $^1$H NMR data of **2** were similar to those of **1** except for the disappearance of the oxygenated methine in **2** (Table 1). In addition, H-4 ($\delta_H$ 7.49) and H-8(12) ($\delta_H$ 8.11) in **2** were deshielded ($\delta_H$ 6.41 and 7.49, respectively in **1**). The above data suggested that the oxygenated methine was replaced by a ketone group in **2**, which was further confirmed by HMBC correlations from H-8(12) to the carbon of this ketone group ($\delta_C$ 184.0). Detailed analysis of 2D NMR spectra of **2** revealed that the remaining substructures of **2** were identical to that of **1**. The trivial name coniofuroic acid B is given to compound **2**.

All isolated compounds were submitted for bioassay against the L5178Y mouse lymphoma cell line but proved to be inactive when tested at an initial concentration of 10 μM.

## ACKNOWLEDGEMENTS

This project was funded by the Deutsche Forschungsgemeinschaft (project number 270650915, GRK 2158). Further support by the Manchot Foundation to P. P. is gratefully acknowledged. T. K. was supported by the National Research, Development and Innovation Office (K120181) and A. M. by the János Bolyai Research Scholarship of the Hungarian Academy of Sciences. The Governmental Information-Technology Development Agency (KIFÜ) is acknowledged for CPU time.

## ORCID

*Attila Mándi* https://orcid.org/0000-0002-7867-7084
*Tibor Kurtán* https://orcid.org/0000-0002-8831-8499
*Zhen Liu* https://orcid.org/0000-0003-3314-7853

## REFERENCES

1. Aly AH, Debbab A, Kjer J, Proksch P. Fungal endophytes from higher plants: a prolific source of phytochemicals and other bioactive natural products. *Fungal Diversity*. 2010;41:1-16.
2. Strobel GA. Endophytes as sources of bioactive products. *Microbes Infect*. 2003;5(6):535-544.
3. Hawksworth DL, Rossman AY. Where are all the undescribed fungi? *Phytopathology*. 1997;87(9):888-891.
4. Frank M, Özkaya FC, Müller WEG, et al. Cryptic secondary metabolites from the sponge-associated fungus *Aspergillus ochraceus*. *Mar Drugs*. 2019;17:99.
5. Abdel-Wahab NM, Scharf S, Özkaya FC, et al. Induction of secondary metabolites from the marine-derived fungus *Aspergillus versicolor* through co-cultivation with *Bacillus subtilis*. *Planta Med*. 2019;85(6):503-512.
6. Abdelwahab MF, Fouad MA, Kamel MS, et al. Tanzawaic acid derivatives from freshwater sediment-derived fungus *Penicillium* sp. *Fitoterapia*. 2018;128:258-264.
7. Elsebai MF, Nazir M, Kehraus S, et al. Polyketide skeletons from the marine alga-derived fungus *Coniothyrium cereale*. *Eur J Org Chem*. 2012;2012:6197-6203.
8. Elsebai MF, Kehraus S, Lindequist U, et al. Antimicrobial phenalenone derivatives from the marine-derived fungus *Coniothyrium cereale*. *Org Biomol Chem*. 2011;9(3):802-808.
9. Ondeyka JG, Zink D, Basilio A, et al. Coniothyrione, a chlorocyclopentandienylbenzopyrone as a bacterial protein synthesis inhibitor discovered by antisense technology. *J Nat Prod*. 2007;70(4):668-670.
10. Schüffler A, Liermann JC, Opatz T, Anke T. Elucidation of the biosynthesis and degradation of allantofuranone by isotopic labelling and fermentation of modified precursors. *ChemBioChem*. 2011;12(1):148-154.
11. Xu J, Aly AH, Wray V, Proksch P. Polyketide derivatives of endophytic fungus *Pestalotiopsis* sp. isolated from the Chinese mangrove plant *Rhizophora mucronata*. *Tetrahedron Lett*. 2011;52:21-25.
12. Kjer J, Debbab A, Aly AH, Proksch P. Methods for isolation of marine-derived endophytic fungi and their bioactive secondary products. *Nat Protoc*. 2010;5(3):479-490.
13. Ashour M, Edrada R, Ebel R, et al. Kahalalide derivatives from the Indian sacoglossan mollusk *Elysia grandifolia*. *J Nat Prod*. 2006;69(11):1547-1553.
14. MacroModel. Schrödinger LLC, 2015. http://www.schrodinger.com/MacroModel.
15. Chai JD, Head-Gordon M. Systematic optimization of long-range corrected hybrid density functionals. *J Chem Phys*. 2008;128:084106.
16. Peverati R, Truhlar DG. Communication: A global hybrid generalized gradient approximation to the exchange-correlation functional that satisfies the second-order density-gradient constraint and has broad applicability in chemistry. *J Chem Phys*. 2011;135:191102.
17. Frisch MJ, Trucks GW, Schlegel HB, et al. *Gaussian 09, Revision E.01*. Gaussian Inc: Wallingford CT; 2013.
18. Stephens PJ, Harada N. ECD cotton effect approximated by the Gaussian curve and other methods. *Chirality*. 2010;22(2):229-233.
19. Varetto U. Molekel 5.4. 0.8. Swiss National Supercomputing Centre, Manno, Switzerland 2009.
20. Superchi S, Scafato P, Gorecki M, Pescitelli G. Absolute configuration determination by quantum mechanical calculation of chiroptical spectra: basics and applications to fungal metabolites. *Curr Med Chem*. 2018;25:287-320.
21. Mándi A, Kurtán T. Applications of OR/ECD/VCD to the structure elucidation of natural products. *Nat Prod Rep*. 2019;36:889-918.
22. Pescitelli G, Bruhn T. Good computational practice in the assignment of absolute configurations by TDDFT calculations of ECD spectra. *Chirality*. 2016;28(6):466-474.

23. Grauso L, Teta R, Esposito G, Menna M, Mangoni A. Computational prediction of chiroptical properties in structure elucidation of natural products. *Nat Prod. Rep.* 2019;36(7):1005-1030.
24. Sun P, Xu DX, Mándi A, et al. Structure, absolute configuration, and conformational study of 12-membered macrolides from the fungus *Dendrodochium* sp. associated with the sea cucumber *Holothuria nobilis* Selenka. *J Org Chem*. 2013;78:7030-7047.
25. Mándi A, Swamy MMM, Taniguchi T, Anetai M, Monde K. Reducing molecular flexibility by cyclization for elucidation of absolute configuration by CD calculations: daurichromenic acid. *Chirality*. 2016;28:453-459.
26. Brémond É, Savarese M, Su NQ, et al. Benchmarking density functionals on structural parameters of small-/medium-sized organic molecules. *J Chem Theory Comput*. 2016;12:459-465.
27. Tran-Cong NM, Mándi A, Kurtán T, et al. Induction of cryptic metabolites of the endophytic fungus *Trichocladium* sp. through OSMAC and co-cultivation. *RSC Adv*. 2019;9:27279-27288.
28. Batista ANL, dos Santos FM Jr, Batista JM Jr, Cass QB. Enantiomeric mixtures in natural product chemistry: separation and absolute configuration assignment. *Molecules*. 2018;23:492.
29. Tóth B, Liktor-Busa E, Kúsz N, et al. Phenanthrenes from *Juncus inflexus* with antimicrobial activity against methicillin-resistant *Staphylococcus aureus*. *J Nat Prod*. 2016;79:2814-2823.
30. Ancheeva E, Mándi A, Király SB, et al. Chaetolines A and B, pyrano [3,2-f] isoquinoline alkaloids from cultivation of *Chaetomium* sp. in the presence of autoclaved *Pseudomonas aeruginosa*. *J Nat Prod*. 2018;81(11):2392-2398.

## SUPPORTING INFORMATION

Additional supporting information may be found online in the Supporting Information section at the end of this article.

**How to cite this article:** Tran-Cong NM, Mándi A, Király SB, et al. Furoic acid derivatives from the endophytic fungus *Coniothyrium* sp.. *Chirality*. 2020;32:605–610. https://doi.org/10.1002/chir.23209